PAPER • OPEN ACCESS

Identification of the wave speed and the second viscosity of cavitation flows with 2D RANS computations - Part I

To cite this article: J Decaix *et al* 2015 *J. Phys.: Conf. Ser.* **656** 012060

View the article online for updates and enhancements.

Identification of the wave speed and the second viscosity of cavitation flows with 2D RANS computations – Part I

J. Decaix[a,1]**, S. Alligné**[b]**, C. Nicolet**[b]**, F. Avellan**[c]** and C. Münch**[a]

[a]University of Applied Sciences and Arts, Western Switzerland, Switzerland.
[b]Power Vision Engineering Sàrl, Ecublens, Switzerland.
[c]Laboratory for Hydraulic Machines, Ecole Polytechnique Fédérale de Lausanne, Switzerland.

Email : jean.decaix@hevs.ch

Abstract. 1D hydro-electric models are useful to predict dynamic behaviour of hydro-power plants. Regarding vortex rope and cavitation surge in Francis turbines, the 1D models require some inputs that can be provided by numerical simulations. In this paper, a 2D cavitating Venturi is considered. URANS computations are performed to investigate the dynamic behaviour of the cavitation sheet depending on the frequency variation of the outlet pressure. The results are used to calibrate and to assess the reliability of the 1D models.

1. Introduction
1D hydro-electric models are used to investigate the dynamic behaviour of hydro-power plants. Particularly, the behaviour at off-design operating points of Francis turbines is of main interest since hydraulic power plants are more and more used to stabilize the electrical power network. To increase the reliability of the 1D model, the parameters involved in the models have to be calibrated.

This paper deals with the development of a methodology to calibrate 1D cavitation models by using results provided by CFD computations. A 2D Venturi geometry [1] is considered. An unsteady pressure condition is set at the outlet. Depending on the frequency of the outlet pressure, the response of the cavitation sheet is analysed.

2. Case study
The test case consists of a Venturi geometry [1] characterized by a divergent angle of 4 degrees (see Figure 1). The inlet velocity is equal to C_{in} = 10.8 m/s (Q_{in} = 0.024 m³/s). At the experimental point, the cavitation sheet develops from the throat and extends approximately 0.08 meter downstream of the throat.

3. 1D modelling of cavitation dynamics
The 1D model is the one developed in the SIMSEN software [2]. For a cavitating flow, the mass conservation equation and the momentum equation write:

---

[1] To whom any correspondence should be addressed.

$$-\frac{dV_c}{dt} = \chi\,\frac{dQ_1}{dt} + C_c\,\frac{dh}{dt} \tag{1}$$

$$\frac{1}{gA}\frac{\partial Q}{\partial t} + \frac{Q}{gA^2}\frac{\partial Q}{\partial x} - \frac{Q^2}{gA^3}K_x + \frac{\partial h}{\partial x} + \frac{\tau_0 \pi D}{\rho gA} - \frac{\mu''}{\rho gA}\frac{\partial^2 Q}{\partial x^2} = 0 \tag{2}$$

With V_c the cavity volume (m^3), Q the discharge (m^3 s^{-1}), χ the mass flow gain factor (s), C_c the cavitation compliance (m^2), g the gravitational acceleration (m s^{-2}), A the cross section (m^2), K_x the gradient of the pipe section (m), h the piezometric head (m), τ_0 the tangential component of the stress tensor (Pa), D the pipe diameter (m) and μ'' is the second viscosity (Pa s). The cavitation compliance C_c is related to the local wave speed whereas μ'' introduces dissipation due the phase change.
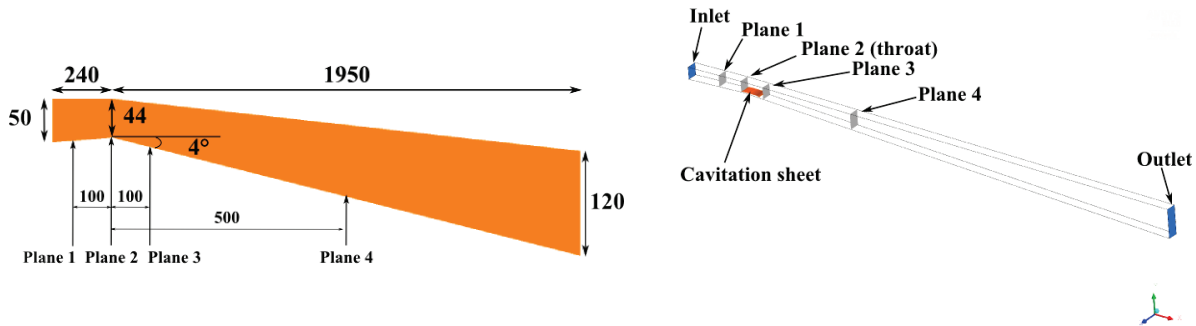

Figure 1: 2D (left) and 3D (right) views of the Venturi.

4. Flow numerical simulation set up

Unsteady cavitating RANS computations are performed with ANSYS CFX 15.0. The two-phase flow is computed using a homogeneous approach. Turbulence is modeled using the k-ω SST model, whereas cavitation is modeled using a transport equation for the vapour volume fraction with the source term based on the simplified Rayleigh-Plesset equation. The pressure vapour is set to p_{vap} = 2'300 Pa. The two parameters of the cavitation model are set to their default value: F_v = 50 and F_c = 0.01. The computations are performed on a 2D computational domain discretized with a structural mesh composed of almost 40'000 nodes. A node is set in the depth since ANSYS CFX is based on the finite volume method. The depth is arbitrary taken equal to 0.044 m.

The discharge is fixed at the inlet to the experimental value Q_{in} = 0.024 m^3/s. Non-slip walls are considered and a symmetry condition is imposed on the side walls. The outlet pressure is provided using a sinusoidal profile. The dimensionless outlet piezometric head h_{out}^* is:

$$h_{out}^* = h_{ref}^* + h_a\,sin(2\pi ft) \tag{3}$$

With: h_{ref}^* = 1.22 and h_a = 0.034 ($h^* = p/(\rho C_{ref}^2/2g)$). Two frequencies are investigated: f = 2 Hz and f = 8 Hz. The time step is set to Δt = 10^{-4} s and the time duration of each simulation is equal to 3 seconds.

5. Dynamic behaviour of the cavity

The cavity volume variation depends on the outlet pressure frequency. Figure 2 (left) shows the outlet and Plane 3 pressure time history. For the highest frequency, the pressure amplitude is almost the same at the outlet and at the plane 3. On the contrary, for the lowest frequency, the amplitude at plane 3 is ten times larger, which corresponds to resonance. Figure 2 (right) shows the cavitation volume time history. For the highest frequency, the cavity volume fluctuates slightly, whereas for the lowest frequency, the cavity volume fluctuates strongly. The low frequency corresponds approximately to the resonance frequency.
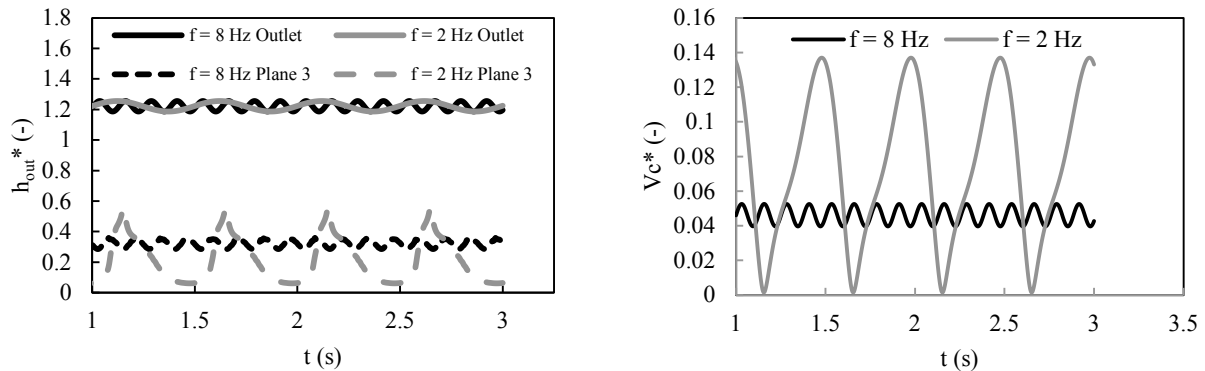
Figure 2: Left: Dimensionless piezometric head time history at the plane 3 and the outlet. Right: Dimensionless volume of vapour time history. Unsteady RANS computations.
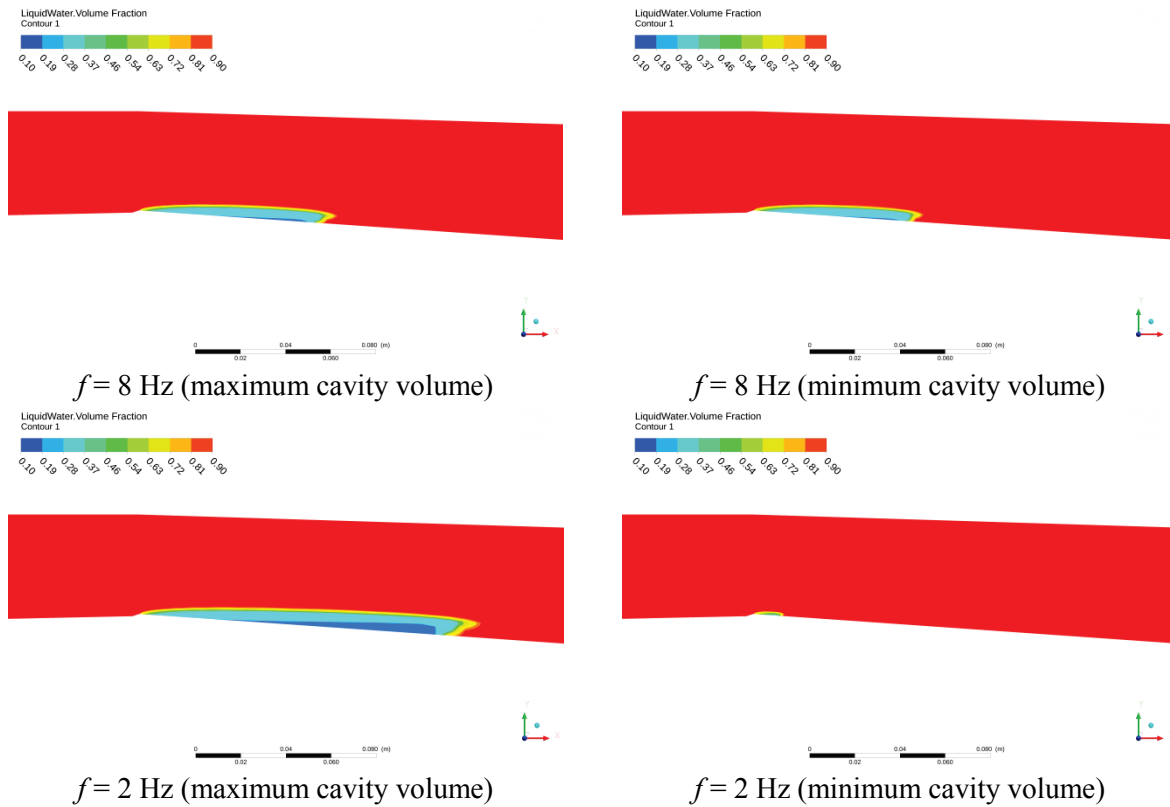

f = 8 Hz (maximum cavity volume)   *f* = 8 Hz (minimum cavity volume)

f = 2 Hz (maximum cavity volume)   *f* = 2 Hz (minimum cavity volume)

Figure 3: Contours of the liquid volume fraction at the minimum and maximum cavity volume for the two frequencies investigated.

The contours of the volume liquid fraction are displayed on Figure 3 for the two frequencies at the minimum and maximal cavity volume. For the highest frequency, the size and the shape of the cavity are rather the same. For the lowest frequency, the minimum of the cavity volume correspond to a small cavitation sheet close to collapse.

The dimensionless streamwise velocity contours are shown on Figure 4. A re-entrant jet is noticeable at the cavity closure except at the minimum cavity volume for the frequency of 2 Hz. For unforced unsteady configurations, the re-entrant jet flows upstream until the cavitation sheet collapses, which can lead to the resonance. The unsteady outlet condition allows controlling and reproducing such a behavior.
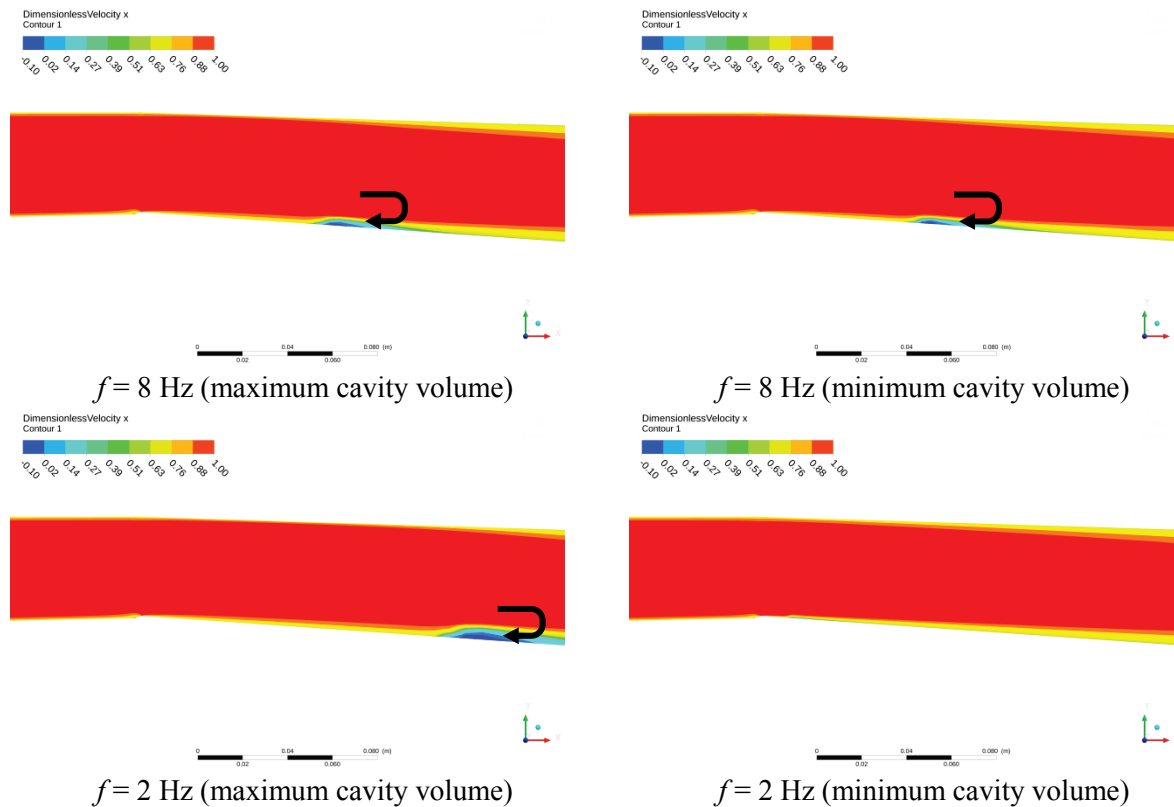
Figure 4: Contours of the dimensionless streamwise velocity at the minimum and maximum cavity volume for the two frequencies investigated. The black arrow refers to the re-entrant jet.

6. Conclusion

The cavitating URANS computations capture the resonance of a cavitation sheet by setting a periodic outlet pressure. The dynamic behaviour of the cavitation sheet can then be used to determine the cavitation compliance C_c and the second viscosity μ'' by matching the cavitation volume fluctuations predicted by the 1D model with the ones provided by the RANS computations [3].

7. References

[1]   Barre S., Rolland J., Boitel G., Goncalves E., and Patella R. F., "Experiments and modeling of cavitating flows in venturi: attached sheet cavitation", *Eur. J. Mech. - B/Fluids*, vol. 28, no. 3, pp. 444–464, May 2009.

[2]   Alligné S., Nicolet C., Tsujimoto Y., and Avellan F., "Cavitation Surge Modelling in Francis Turbine Draft Tube", *J. Hydraul. Res.*, vol. 52, no. February 2015, pp. 1–13, 2014.

[3]   Alligné S., Decaix J., Nicollet C., Avellan F. and Münch C., "Identification of the wave speed and the second viscosity in cavitating flow with 2D RANS computations – Part II". In *Proc of the 9th International Symposium on Cavitation CAV 2015*, 6-10 Dec 2015, Lausanne, Switzerland.

Acknowledgments